Absolute Integral and Differential Cross Sections for the Reactive Scattering of $H^- + D_2$ and $D^- + H_2$

E. Haufler, S. Schlemmer, and D. Gerlich*

Institut für Physik, Gasentladungs- und Ionenphysik, TU Chemnitz, 09107 Chemnitz, F. R. Germany

Received: February 26, 1997; In Final Form: May 5, 1997[⊗]

For the two reactions $H^- + D_2 \rightarrow D^- + HD$ and $D^- + H_2 \rightarrow H^- + HD$, absolute integral and differential cross sections have been determined in a guided ion beam (GIB) apparatus. From the effective cross sections, measured in the translational energy range $E_T = 0.1-10$ eV, thresholds for the onset of the reactions have been derived, indicating effective barrier heights of 350 ± 60 meV for $H^- + D_2$ and 330 ± 60 meV for $D^- + H_2$. These values are substantially lower than previously reported experimental and theoretical data. Comparison of the integral cross sections for the two isotopic variants reveals a significant isotope effect. The collision of the light ion with the heavy molecule leads to a cross section which is almost a factor of 2 smaller than for D^- reacting with H_2. Possible experimental effects discriminating D^- versus H^- are discussed. The recently reported differential cross section for $H^- + D_2$ which has been obtained with a crossed beam experiment is in good accordance with the present data determined with the GIB technique. A new result is that, at small collision energies, the angular dependence is very similar for both isotopic variants. In view of the quite large isotopic effect for the integral cross sections this is not self-evident. All these detailed results pose a challenge to full quantum dynamical scattering theory of the H_3^- collision system.

Introduction

Collisions of positive, neutral, or negatively charged hydrogen atoms with hydrogen molecules belong to the most fundamental molecular systems and, therefore, are interesting test objects for detailed dynamical studies. In the $H^+ + H_2$ case, the interaction is dominated by the strongly bound H_3^+ intermediate, whereas the interaction of H or H^- with H_2 is predominantly determined by a barrier. At chemical distances, the potential energy surface of H_3^- is very similar to that of H_3, including anisotropy, barrier height, and other characteristics. The reason is that the additional electron in H_3^- is located at rather large distances from all nuclei, and as a consequence, the main interaction is given by the three nuclei and the three "inner" electrons. At larger $H^- - H_2$ distances, the charge-induced dipole interaction leads to a shallow well. Another significant difference between the neutral and the negative system is that the fourth electron gives rise to additional reaction channels involving electron detachment.

For a quantitative theoretical description of experimental data reliable potential energy surfaces (PES) are necessary. The most recent, accurate ab initio PES has been determined by Stärck and Meyer employing MR-CI and CEPA(2) calculations for 403 nuclear configurations.[1] The reaction path of minimal energy is given for the linear approach and shows a barrier height of 458 meV (zero-point energy not included). A linear H_3^- complex with four bound vibrational levels has been found for the $H^- + H_2$ system. The electron detachment seam has been determined by the authors with the lowest point to be in the perpendicular geometry requiring an energy of 1.2 eV. The similarity to the neutral system and the additional competition between reaction and electron detachment makes the H_3^- system a challenge to state-of-the-art scattering theory. Most recently state-to-state reaction probabilities for the rearrangement reaction have been calculated by Belyaev et al.[2] by the **S**-matrix Kohn variational method for the collinear configuration and by Mahapatra et al.[3] using the time-dependent wave packet approach.

At total energies below the dissociation limit of hydrogen, the outcome of an $H^- + D_2$ collision can be inelastic excitation (1), rearrangement (2), and electron detachment, without (3) or including a rearrangement (4):

$$H^- + D_2 \rightarrow H^- + D_2(v',J') \quad (1)$$

$$\rightarrow D^- + HD(v',J') \quad (2)$$

$$\rightarrow H + D_2(v',J') + e^- \quad (3)$$

$$\rightarrow D + HD(v',J') + e^- \quad (4)$$

These are important mechanisms in hydrogen discharges and H^- sources. However, compared to the neutral reaction system $H + H_2$, there have been only a few experimental studies. For the determination of the threshold energy, which is associated with the presence of a barrier, integral cross sections $\sigma(E)$ are very sensitive to probe this characteristic feature of the PES. Up to recently only two sets of data were available from Michels and Paulson[4] using a tandem mass spectrometer and Huq et al.[5] using a trap employing a combination of an electrostatic and a magnetic field. The discrepancy between these two measurements bearing on the determination of the integral cross section could be resolved by crossed beam studies of the $H^- + D_2$ reaction by the group of Linder,[6] who also recently reported interesting details on rotational excitation in $H^- + H_2$ collisions.[6] In the reactive H−D exchange reaction, the angular distribution of the D^- products is strongly forward peaked, which indicates that the reaction occurs preferentially for a collinear configuration of the reactants similarly to the $H + H_2$ reaction. By integrating over angles and summing over partial cross sections (product vibrational states) integral cross sections have been determined. Absolute units are obtained from a comparison to elastic $H^- + He$ scattering. These authors find a threshold energy for the reactive channel of $H^- + D_2$ of 420 ± 120 meV which is in good agreement with the proposed value of Stärck and Meyer[1] of 490 meV (including zero-point energies). Here

[⊗] Abstract published in *Advance ACS Abstracts,* July 15, 1997.

S1089-5639(97)00724-X CCC: $14.00

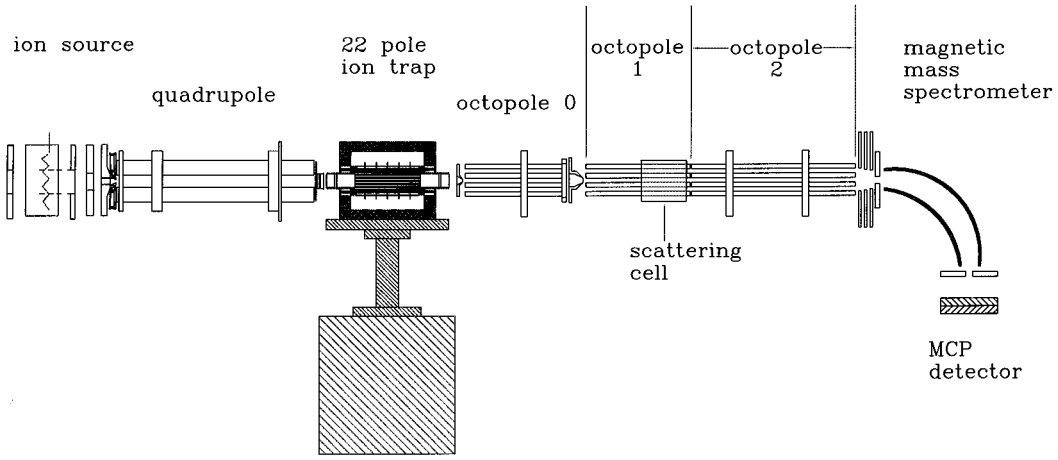

Figure 1. Guided ion beam apparatus with integrated 22-pole ion trap. H^- or D^- ions, formed by electron bombardment of methane, are thermalized in the trap before they are transferred via octopole 0 to octopole 1. In this ion guide, which is surrounded by a scattering cell, the ions react with the target gas. Octopole 2 is utilized for TOF analysis. The ions are mass analyzed in a magnetic 90° mass spectrometer and detected with an MCP detector.

we present results obtained with a guided ion beam (GIB) apparatus for the rearrangement reaction (2) and its isotopic variant (6):

$$D^- + H_2 \rightarrow D^- + H_2(v',J') \quad (5)$$

$$\rightarrow H^- + HD(v',J') \quad (6)$$

After a short description of the experimental setup, integral, and differential cross sections are reported and discussed with respect to isotope effects, threshold behavior, and other details of the reaction dynamics.

Experimental Section

The measurements have been performed in the universal guided-ion beam apparatus shown in Figure 1. A thorough description of this machine, of the components and of the routinely performed test procedures is given elsewhere.[7] In addition to the previously described apparatus a 22-pole ion trap for thermalizing the reactant ions has been added in the current setup. Some more details, especially concerning the determination of product velocities have been published recently.[8] H^- or D^- ions were created by electron impact of CH_4 (respectively CD_4) in a simple standard ion source using an electron energy of 50 eV and a precursor gas pressure of typically 10^{-4} mbar. The produced negatively charged ions were transferred into a 22-pole ion trap via a quadrupole, operated as a mass filter in a low pass mode. To improve the kinetic energy distribution the ions have been stored for 5−10 ms in a 20 K ion trap. According to our experience with this trap, collisions with the ambient cold H_2 (or D_2) buffer gas (density $\sim 10^{13}$ cm^{-3}) usually lead to a fast relaxation of the velocity distribution. In this way a pulsed beam of ions with a repetition period of 10 ms, a pulse width of 30−50 μs, and an intensity of about 50 ions/pulse has been obtained.

From the trap, the ions are transferred via octopole 0 into octopole 1 (length 13.6 cm, inner diameter 0.6 cm) which guides them into and through the scattering cell (see Figure 1, effusive target gas at 300 K). Primary ions and products enter then the 46.8 cm long octopole 2, which allows us to determine both the axial and the transverse velocity of the product ions. Octopoles 1 and 2 are coupled to the same RF source but can be operated with different dc bias. Usually octopole 2 is floated 0.5 V below octopole 1 in order to avoid reflections of slow ions in the transition region or in the long octopole 2. The transmission function of the octopoles has been carefully tested using positive H^+, D^+, and H_2^+ ions. Operating conditions were a frequency of $\Omega = 2\pi 16.7$ MHz and an amplitude of $V_0 = 80$ V. Since the effective potential is proportional to the square of the charge, these results are directly applicable to the negative ions H^- and D^-. Therefore, we are rather sure that the operating conditions of the octopoles 1 and 2 are sufficient to provide 4π collection efficiency for the reaction products.

At the end of octopole 2 the ions leave the beam guiding system and are accelerated up to $E = 3.5$ keV by an electrostatic system and then focused onto the entrance slit of the 90° magnetic mass analyzer. Finally the mass-analyzed ions hit the surface of a microchannel plate detector at an energy of about 2 keV. The electric pulses are processed and counted in the usual way. The absolute values of the cross sections are determined from count rates, target gas density, and the effective length of the scattering cell. The largest error in absolute cross sections originates from the determination of the target gas density (∼20%) and the detection efficiency.

It recently has been reported[9] that for both positive hydrogen ions, H^+, and D^+, the detection efficiency is equal to 41%. The situation for H^- and D^- is still unclear and will be discussed below. In comparison the error in collection efficiency is negligible.

One of the goals of the present work was to determine the influence of the barrier and the importance of tunneling for this prototype reaction. Therefore it was very important to account for experimental artifacts which can lead to a product signal at energies below the threshold, e.g., thermal motion of the 300 K target gas. Unfortunately, the largest perturbation was due to the kinetic energy distribution of the primary beam. This distribution was not given by the thermal distribution in the low temperature ion trap but it was much wider. Possible explanations for this are effects of RF heating in transition regions, for example during the extraction of the ions from the trap or during the injection into octopole 0. For a discussion concerning the influence of these RF-DC transition regions see ref 8. For analyzing the experimental results, the energy distribution of the ions in the interaction region has been measured very carefully using TOF analysis. One of the results is shown in Figure 2. The main part of the distribution can be fitted with a Gaussian (solid line) with an energy spread of 220 meV (fwhm); however, also the low-intensity tail extending to higher energies must be accounted for as will be seen below.

The primary ion beam was always operated in a pulsed mode.

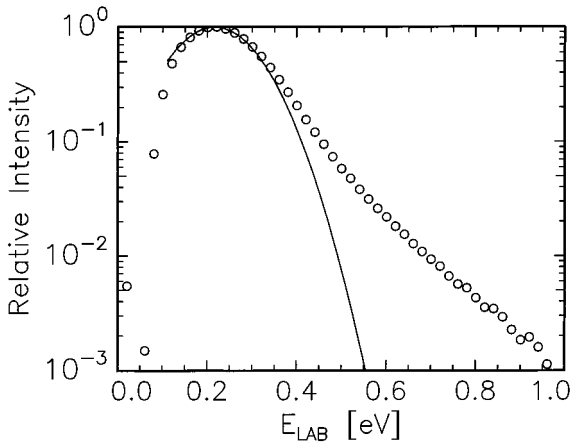

Figure 2. Energy distributions of primary H^- ions determined via TOF analysis. The solid line represents a Gaussian fit with a fwhm of 220 meV. The log scale has been chosen in order to emphasize the high-energy tail which has to be accounted for in the evaluation of the measured threshold onset of the reaction.

This allows us not only to precisely calibrate the kinetic energy distribution of the primary ions by time-of-flight (TOF) but also to determine arrival times of product ions. TOF spectra are recorded by a multichannel scaler with a typical dwell time of 2 μs. Up to 10^6 ion pulses/spectrum are accumulated. Thus spectra are obtained even for very weak signal rates at energies below the threshold. The product TOF distributions are transformed into axial velocity spectra which are identical with the differential cross section $d\sigma/dv_{1p}'$, where v_{1p}' denotes the velocity component of the products along the axis of the octopole (laboratory frame). By variation of the strength of the guiding RF field, doubly differential cross sections $d^2\sigma/dv_{1p}'$ dv_{1t}' can be obtained. v_{1t}' is the corresponding perpendicular velocity component of v_1'. In this paper most of the information on the collision dynamics can be derived from the axial product velocity distributions alone. The possibilities and limitations of this GIB-TOF method is thoroughly discussed in refs 7 and 8. For a detailed discussion of the scattering kinematics including the influence of the target motion see ref 10.

Results and Discussion

I. Integral Cross Sections. Integral cross sections for the rearrangement reaction have been measured for the two isotopic variants $H^- + D_2$ and $D^- + H_2$. Results are presented in Figure 3 as a function of collision energy in the range of 100 meV to 10 eV (E_T: translational energy in the center-of-mass system). Both curves show an onset at about 0.3 eV, a maximum around 1 eV, followed by a decrease at larger collision energies. This general behavior can be related to the basic features of the PES. A threshold is expected due to the barrier at 0.45 eV. This onset of reactivity is similar to the one observed for the neutral $H + H_2$ reaction. However, in contrast to this prototype reaction the decrease of the cross section for the title reaction has to be related to the competition with another reaction channel, i.e., electron detachment.[3,4] The onset of this decrease is in accord with the calculation of Stärck and Meyer who predict that $H^- + H_2 \rightarrow H + H_2 + e^-$ opens up at 1.2 eV. It is gratifying to see that the main features of the PES appear in the behavior of the integral cross section. In addition the general trend observed for the two isotopic variants is very similar, as expected. However, the fact that the cross section for the heavy ion colliding with the light molecule is larger by a factor of 2 is quite surprising. Accounting for the zero-point energies leads only to 50−80 meV difference in barrier height which cannot

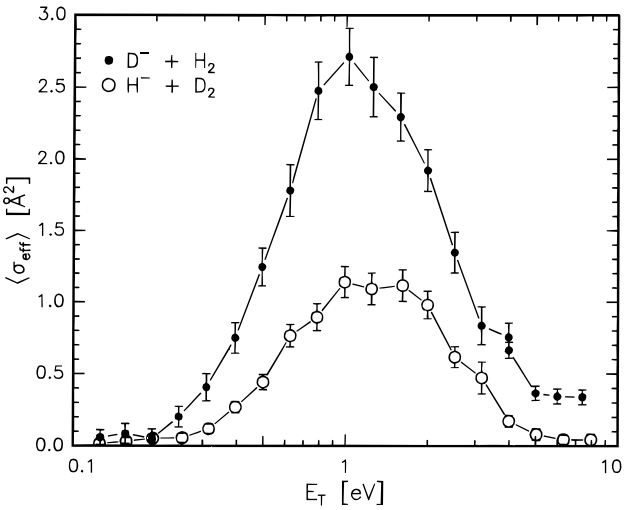

Figure 3. Integral cross section σ for the $H^- + D_2$ (○) and the $D^- + H_2$ (●) rearrangement reaction as a function of collision energy E_T (translational energy in the center-of-mass system). The error bars account only for the statistical uncertainty. Although similar in shape the curves differ by more than a factor of 2 which indicates a considerable isotopic effect.

explain this large isotope effect. Also an earlier onset of the electron detachment channel for $H^- + D_2$ cannot be responsible for this effect since Huq et al.[5] measure only small cross sections for the detachment channel at these energies. In addition they derive a later onset for $H^- + D_2$ (1.45 eV) than for $D^- + H_2$ (1.20 eV), however with a slightly steeper slope in the case of $H^- + D_2$.

To determine absolute cross sections great care has been taken to avoid a mass-dependent transmission in the guiding field of the apparatus as well as in the magnetic mass spectrometer. This has been thoroughly checked as discussed in the Experimental Section. Therefore only the possibility of a large difference in detection efficiency of the microchannel plate detector (MCP) for D^- as compared to H^- could account for a larger experimental error. Unfortunately nothing is known about the absolute detection efficiency of MCP detectors for these two negative ions; however, it can be expected that the detection efficiency is comparable to the positive ion or neutral. It should be noted that our MCP detector was operated with an amplifier and discriminator for particle counting. Although minor experimental effects cannot be ruled out the large isotope effect observed is significant. An even larger isotopic enhancement of a factor 3 to 4 for $D^- + H_2$ has been reported previously by Michels and Paulson;[4] however, this early experiment faced several problems concerning the transmission and collection of product ions, and it is questionable whether part of the isotopic effect has to be attributed to mass-selective discrimination.

Figure 4 shows a comparison of the results of Michels and Paulson,[4] Huq et al.,[5] and Zimmer and Linder[6] with our data for $H^- + D_2$. The discrepancies to Michels and Paulson[4] are quite dramatic due to the problems mentioned. In the experiment of Huq et al.[5] no mass separation was available; therefore D^- reaction products and inelastically scattered H^- were detected likewise. The authors state that the values given for the integral cross sections serve as an upper limit only. This is consistent with the results of Zimmer and Linder and our data. In general, the agreement with Zimmer and Linder[6] is good, i.e., the threshold position, the position of the maximum and the decrease for higher collision energies are very similar. It should be noted that for the determination of integral cross sections from crossed-beam experiments integration over the signal obtained at different angles has to be performed. In this

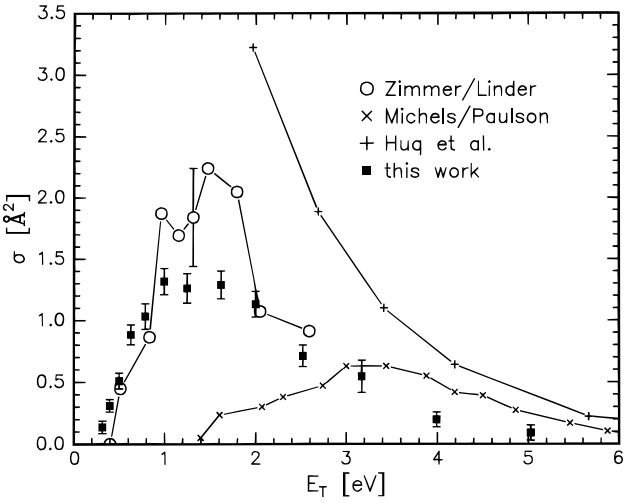

Figure 4. Comparison of the integral cross section for the reaction $H^- + D_2 \rightarrow D^- + HD$ with results from previous work.[4−6] Good agreement is achieved with the results of a crossed beam study by Zimmer and Linder.[6] Note the comparably small error bars of the GIB experiment.

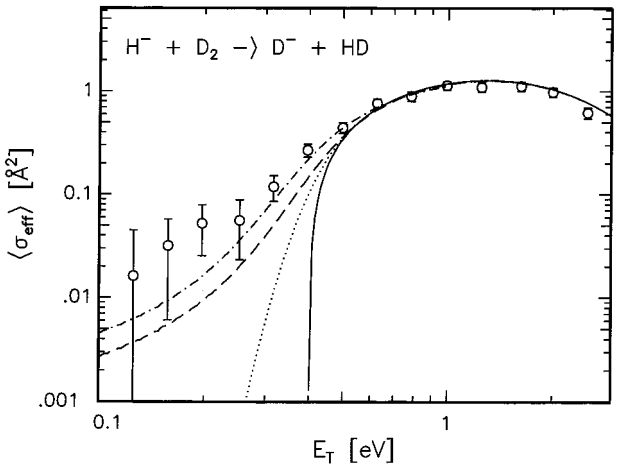

Figure 5. Evaluation of the threshold behavior of the integral cross section of the reaction $H^- + D_2 \rightarrow D^- + HD$. To determine reliable threshold energies, it is necessary to account for the thermal motion of the target gas as well as the finite energy distribution of the primary ions. The solid line is the trial function explained in the text (threshold 400 meV), the dotted line shows the influence of the target motion. The dashed line and the dash−dotted line are the complete simulation, assuming a threshold of 400 and 350 meV, respectively.

process the finite angle of acceptance and the effective interaction volume have to be accounted for which give rises to larger uncertainties. In contrast the octopole ion guide incorporates a 4π integration leading to a 100% collection efficiency within an uncertainty of less than 5%.

For a quantitative comparison of the threshold position and the absolute values of the integral cross section several details of our GIB experiment have to be discussed. It can be seen from Figure 3 that the integral cross section does not show a clear-cut threshold position but a prolonged onset in the range 0.25−0.4 eV. This smearing out is due to the finite energy distribution of the primary ions and due to the thermal motion of the target gas. To account for these influences and determine the threshold position precisely, we used an analytical expression for the integral cross section as input for a full simulation of the broadening caused by the experimental conditions. The result of this simulation is given in Figure 5 together with the experimental data in a logarithmic plot of the integral cross section as a function of the collision energy. In our model we used the simple expression

$$\sigma(E_T) = \begin{cases} \mathbf{A}\,(E_T - E_B)e^{-E_T/E_D}, & E_T > E_B \\ 0 & \text{otherwise} \end{cases} \quad (7)$$

for the intrinsic integral cross section $\sigma(E_T)$ where E_T is the collision energy and E_B the threshold position, which is related to the barrier height of the corresponding PES. The constant $A = 6$ Å^2/eV and $E_D = 900$ meV have been adjusted to the experimental data to reproduce $\sigma(E_T)$ at elevated energies. The solid line in Figure 5 shows this analytical expression for $E_B = 400$ meV. For calculating the effective cross section $\sigma_{eff}(v_1)$, E_T is substituted by $(\mu/2)g^2$, where g is the relative velocity, $g = |v_1 - v_2|$, v_1 denotes a well-defined velocity of the colliding primary ion, and v_2 is the velocity of the target molecule. In the case of a scattering cell, the velocity distribution of the target molecules is a thermal distribution, and the distribution of the relative velocity is given by the well established generalized Maxwell−Boltzmann distribution, $f^*(g;v_1,T_2)$,[11] where T_2 is the temperature of the target gas and $v_1 = |v_1|$. Thus, the effective integral cross section can be written as

$$\sigma_{eff}(v_1) = \int_0^\infty dg\ (g/v_1)\sigma(g)\ f^*(g;v_1,T_2) \quad (8)$$

The result of this averaging procedure is shown in Figure 5 as dotted line for a target gas temperature of 300 K and $E_B = 400$ meV. In the present case, this first step of simulation shows a rather small extension of the cross section toward smaller energies, and only a small fraction of the observed broadening effect can be attributed to the finite target gas temperature. To improve the agreement with the experimental data, it is essential to account for the distribution of the primary velocity, $f(v_1)$. This can be done by simply integrating σ_{eff} over v_1:

$$\langle\sigma_{eff}\rangle = \int_0^\infty dv_1\ f(v_1)\ \sigma_{eff}(v_1) \quad (9)$$

This averaged effective cross section (dashed line in Figure 5) accounts fully for the experimental conditions and the agreement with the measured values is much better. Due to the very low signal at small collision energies the relative errors of the experimental cross sections are fairly large. Nevertheless the deviations of the full simulation from the data is significant. For further improvement simulations for smaller threshold energies have been carried out. For example, the dashed−dotted line shows a result of a simulation using $E_B = 350$ meV. This simulation shows a reasonable agreement with experiment, except for the lowest collision energies. Below the threshold tunneling has to be considered; however, due to the fairly large error bars its contribution cannot be evaluated. Comparing our value for E_B with the theoretical threshold of 490 meV, proposed by Stärck and Meyer[1] reveals a large discrepancy. The latter value is not the result of a scattering calculation but represents the barrier height including the zero point energy in the H_3^- transition state derived from the curvature of the PES. This might overestimate the threshold. Concerning experimental artifacts, possible contributions from the proposed[12] excited state of $H^-(^3P)$ have to be discussed; however, since the electron is bound only by 9.5 meV, it seems pretty unlikely that $H^-(^3P)$ can be produced in a considerable amount in an ion source employing electron bombardment. In addition any excited H^- would not survive the collisions in the intermediate thermalization process of the primary ions. In summary we conclude that the predicted barrier height has to be corrected significantly.

Similar data evaluations have been carried out for $D^- + H_2$ and can be found in ref 13. Due to the different mass ratio of

the two reagents the influence of the thermal motion of the target is considerably larger. On the other hand the quality of the primary beam was much better. For this system a threshold energy of $E_B = 330$ meV has been derived. As expected from the differences in zero-point energies, this value is slightly smaller as compared to $H^- + D_2$. Accounting for all experimental errors such as energy calibration, we believe both values to be correct within a margin of 60 meV.

Comparison of the threshold, derived for $H^- + D_2$ from the crossed beam experiment of Zimmer and Linder (420 ± 120 meV), with the GIB result (350 ± 60 meV) shows reasonable agreement within the uncertainties. The strength of the GIB technique with respect to measuring integral cross sections and calibrating the collision energy has already been pointed out. The smaller errors for the threshold energy are an indication of this technical aspect. Another difference of the two experiments is the rotational temperature of the target molecules. In our scattering cell D_2 is held at 300 K. Zimmer and Linder use a molecular beam for which they estimate a rotational temperature of 180 K. The additional rotational energy in the GIB experiment which is about 10 meV would lead to a minor shift in the GIB threshold provided that rotational energy can help to surmount the barrier. In contrast, detailed quasi classical trajectory (QCT) calculations for the neutral system $D + H_2(v = 0,j) \rightarrow H + HD$[14,15] reveal a decrease of the integral cross section in the vicinity of the threshold energy going from $j = 0$ to $j = 4$.

No reliable integral cross sections for the isotopic variants of the title reaction are available for comparison. Since also theoretical predictions are missing, a discussion of the experimentally observed isotope effect is difficult. Fortunately there is the similarity to the neutral reaction for which a comparable isotopic effect has been observed experimentally as well as theoretically. Westenberg and de Haas[16] have reported a 3-fold increased thermal rate coefficient for $D + H_2$ as compared to $H + D_2$ from a flow reactor experiment at 750 K. Note, however, that not only the magnitude of the integral cross section can lead to an increase of the thermal rate coefficient but also a shift of the threshold as observed here for $D^- + H_2$. Therefore the origin of this observed isotope effect remains unclear. Currently Aoiz et al.[17] are carrying out further QCT calculations for the two neutral reactions. At a total energy of 0.8 eV they find the exchange reaction in $D + H_2$ to be favored by about a factor of 2.7 in comparison to $H + D_2$. This factor is quite comparable with our present result. Several aspects of the dynamics of the different variants are discussed one of which being the fact that the velocity of approach to the cone of acceptance is smaller for $D + H_2$, and therefore this system finds more time to orient in order to overcome the barrier. According to Aoiz,[17] the key argument seems to be that the heavier the atom, the more momentum can be transferred to the diatom which induces more vibrational excitation and promotes the reactivity. More detailed calculations at full quantum level are desired in order to resolve this open question.

II. Differential Cross Sections (TOF). In addition to integral cross sections, product time-of-flight (TOF) distributions have been measured for both isotopic variants of the title reaction using octopole 2 (see Figure 1). As has been explained briefly in the Experimental Section and in more detail in ref 8, the flight time is related to the axial component (parallel to the axis of the guiding field) of the products laboratory velocity (v_{1p}'). Results for $H^- + D_2$ at three collision energies are shown in Figure 6. Each velocity distribution is plotted as a function of v_{1p}'. The three plots are arranged such that they are drawn to the same u_{1p}' axis, where u_{1p}' is the parallel component of

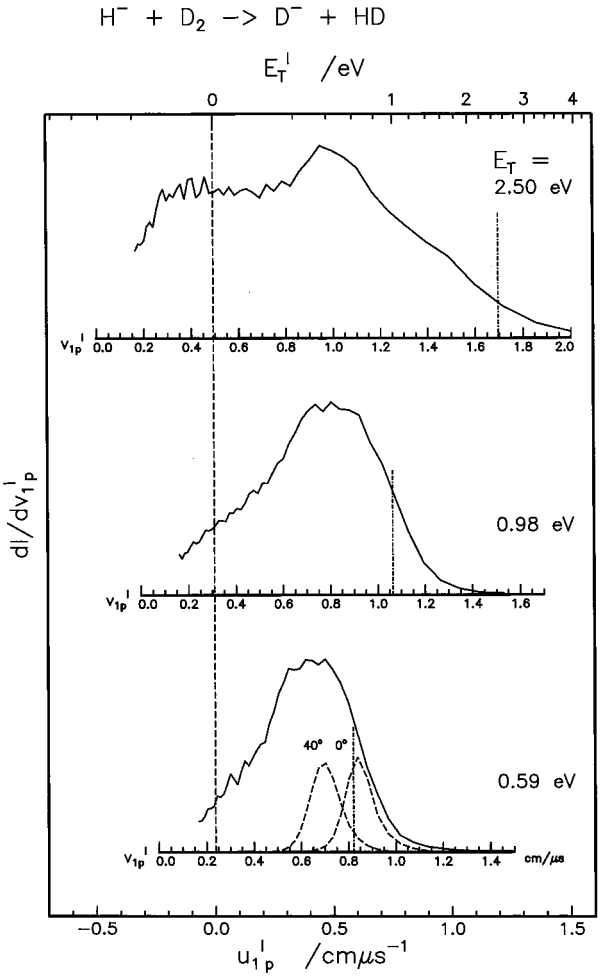

Figure 6. Axial velocity distributions of D^- products at three collision energies. Plots are drawn to the same center of mass (CM) velocity u_{1p}' (bottom scale). The center of mass velocity is marked as the long dashed vertical line. Dashed−dotted lines indicate the position of products which are scattered into forward direction with $\Delta E_T = 0$. The Gaussian like curves illustrate the achievable angular resolution.

center of mass (CM) product velocity after the collision. $u_{1p}' = 0$ denotes the motion of the center of mass (CM) in the laboratory frame and is emphasized by the long vertical dashed line. The difference between $u_{1p}' = 0$ and $v_{1p}' = 0$ is equal to the nominal center of mass velocity. Forward scattered products, i.e., travelling in the direction of the ionic reactant, are characterized by $u_{1p}' > 0$. The upper scale shows the translational energy after the collision, E_T'. The nominal value for the translational exoergicity $\Delta E_T = E_T - E_T' = 0$ (neglecting differences in zero-point energies) is marked by the short vertical dashed−dotted lines. The fact that products are found with even larger CM velocities is due to the thermal motion of the target molecules and to the finite energy distribution of the parent ions.

Starting with the bottom panel at $E_T = 0.59$ eV we find a preference for forward scattering whereas the top panel shows a substantial broadening and shift toward smaller velocities u_{1p}'. This behavior can be related either to internal excitation of the HD product (vibrational excitation up to $v' = 4$, higher rotational states) or to scattering into larger angles which also reduces the axial component of the product velocity. This ambiguity can be removed in the GIB experiment when one records TOF distributions at various guiding field strengths, i.e., RF amplitudes are used for discriminating all those products which have a transverse velocity component, v_{1t}', larger than a certain value. More details on this method can be found in ref 8.

Employing this technique, it has been checked that for $E_T =$

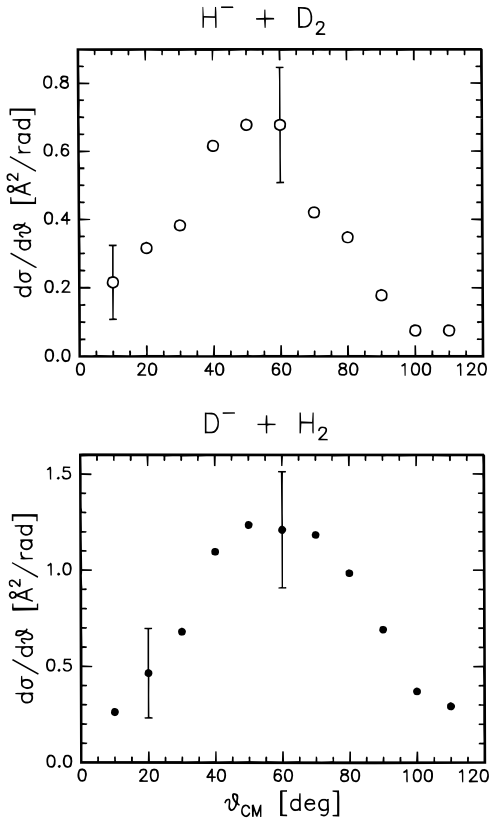

Figure 7. Absolute differential cross sections $d\sigma/d\vartheta$ (concerning $d\sigma/d\omega$ see Figure 8 and eq 10) for the two isotopic variants of the H−D exchange reaction, measured at a collision energy $E_T = 0.6$ eV. The shape of the curves are similar, concerning the magnitude see (also Figure 3).

0.59 eV products are not vibrationally excited and rotation plays only a minor role. Therefore, the shape of the distribution is given simply by the angular distribution of products. Similar observations have been made for $E_T = 0.98$ eV. Under such conditions angular distributions can be determined from the GIB velocity distributions without the big intensity problems common to traditional scattering experiments measuring doubly differential cross sections. To illustrate the resolving power of the GIB technique two angular contributions for $\vartheta_{CM} = 0°$ and $\vartheta_{CM} = 40°$ are plotted in the bottom panel of Figure 6. In this calculation the thermal motion of the target gas as well as the finite energy distribution of the parent ions have been accounted for. This leads to the finite width of the distributions shown.

Angular distributions, i.e., differential cross sections $d\sigma/d\vartheta(\vartheta_{CM})$, have been determined by superimposing angular contributions at increments of $\Delta\vartheta_{CM} = 10°$ and fitting the sum to the experimental velocity distributions shown in Figure 6. Absolute values are given from the calibration of the integral cross sections discussed in the previous section. Results for the lowest collision energy for $H^- + D_2$ as well as $D^- + H_2$ are shown in Figure 7. Both distributions are quite similar. Most of the intensity is scattered in a narrow angular range from about 30° to 90° with a maximum around $\vartheta_{CM} = 60°$. At first sight it seems surprising that the cross sections are small at small scattering angles because inspection of the velocity distributions indicated already a strong forward scattering. However, contributions for small angles (e.g., $\vartheta_{CM} < 20°$) all end up at similar product velocities $v_{1p}' = v_{CM} + u_l' \cos(\vartheta_{CM})$. Therefore these angular distributions are quite typical for forward scattered products.

Due to the similarity of the angular distributions it turns out that the isotopic effect observed for the integral cross section

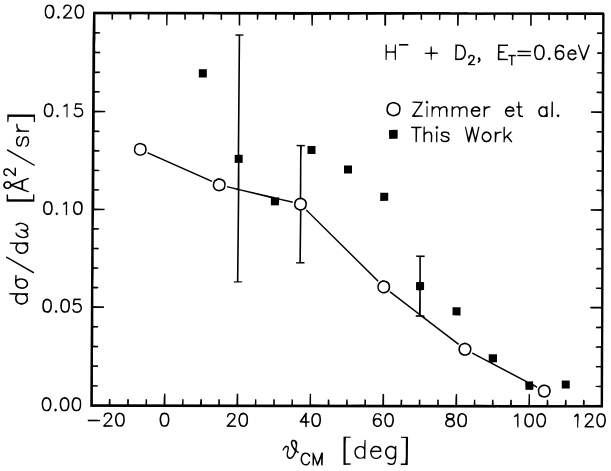

Figure 8. Differential cross sections (here $d\sigma/d\omega$, see eq 10) for the reaction $H^- + D_2 \rightarrow D^- + HD$, measured at a collision energy $E_T = 0.6$ eV. The guided ion beam results from this work (filled squares) are in gratifying agreement with the crossed beam results from Zimmer and Linder (open circles).

cannot be attributed to a different scattering mechanism. Although the experimental uncertainties are quite large it seems that the maximum in $d\sigma/d\vartheta$ is slightly shifted toward larger scattering angles for $D^- + H_2$ (lower panel Figure 7), and the distribution is extending toward larger scattering angles. In the view of this result several aspects regarding the dynamics of this collision system can be addressed. Angular distributions are derived from the measured TOF distributions for $E_T = 0.6$ eV. Only little kinetic energy is available in the vicinity of the barrier. Therefore in both isotopic variants the system will overcome the barrier only in a near-collinear configuration. Starting from this configuration the fraction of the PES probed in the exit channel has to be quite similar for both isotopic variants in order to be consistent with the similarity of the two angular distributions. Therefore the major reason for the increased reactivity of $D^- + H_2$ has to be searched in the dynamics in the entrance channel of the reaction. In addition, the small differences in the differential cross sections could be attributed to the difference in zero point energies, especially in the vincinity of the collinear transition state. These results are consistent with the theoretical results for the neutral system and with the already mentioned mechanistic explanations of Aoiz,[17] who expects the key for the large isotopic effect to be related to the dynamics of the entrance channel. In that respect our new results might serve as a new test case for calculations dealing with the influence of the isotopic constitution of the reactants to the dynamics of the collision.

For a comparison with doubly differential cross sections from Zimmer and Linders' crossed beam experiment the simple relation between $d\sigma/d\omega$ and $d\sigma/d\vartheta$ has to be recalled:

$$\frac{d\sigma}{d\vartheta} = \int_0^{2\pi} d\phi \sin(\vartheta) \frac{d\sigma}{d\omega} = 2\pi \sin(\vartheta) \frac{d\sigma}{d\omega} \qquad (10)$$

In the GIB experiment the integration over the azimutal angle ϕ is included intrinsically. Figure 8 shows a comparison of our results to Zimmer and Linders' differential cross sections for the $H^- + D_2$ reaction at $E_T = 0.6$ eV (note the absolute scale). It is gratifying to see that these two very different experimental techniques lead to very similar cross sections. Experimental uncertainties in the GIB setup amount to a comparably large error for small scattering angles while they are pretty small at intermediate angles. This enhancement of the error is due to the influence of the angular-dependent weight

$2\pi \sin(\vartheta)$. However, this example shows that differential cross sections from a GIB experiment are quite reliable. Although this technique has been commonly accepted to be well suited for the measurement of integral cross sections it should also be considered as a powerful tool for the determination of differential cross sections.

Conclusions

Reliable absolute integral and differential cross sections have been determined for two isotopic variants of the $H^- + H_2$ prototype reaction. Accurate threshold energies could be obtained from these measurement. These values are substantially lower than reported previously. This finding shows that rigorous theoretical investigations for an accurate PES and associated 3D-quantum scattering calculations are needed for this reaction. Integral cross sections show a maximum at approximately 1 eV when the electron detachment channels come into play. For the $D^- + H_2$ variant this maximum is enhanced by a factor of 2 as compared to $H^- + D_2$. This large isotopic effect also bears an explanation from theory. At small collision energies almost no internal excitation (no vibrational and almost no rotational excitation) of the product HD is found in our experiment. This allows a determination of absolute differential cross sections from the measured product velocity distributions. For $H^- + D_2$ we find good agreement of our differential cross sections with the results of Zimmer and Linders' crossed-beam measurements. The angular distributions for the two isotopic variants are quite similar in shape, which is consistent with the assumption that the isotopic effect can be explained from mechanistic considerations in the entrance channel of the reactive collision. From these results it is quite clear that the $H^- + H_2$ reaction and its isotopic variants serves as a protype reaction system, and we hope that it might stimulate improved theoretical investigations which should provide us with theoretical predictions of axial velocity distributions.

Acknowledgment. We like to thank F. Linder and his group for borrowing us their duoplasmatron source for our first experiments and for fruitfull discussions. We thank J. Aoiz for supporting us with information on the reactivity of the different isotopic neutral systems prior to publication.

References and Notes

(1) Stärck, J.; Meyer, W. *Chem. Phys.* **1993**, *83*, 176.
(2) Belyaev, A. K.; Colbert, D. T.; Groenenboom, G. C.; Miller, W. H. *Chem. Phys. Lett.* **1993**, *209*, 309.
(3) Mahapatra, S.; Sathyamurthy, N. *J. Phys. Chem.* **1996**, *100*, 2759.
(4) Michels, H. H.; Paulson, J. F. In: *Potential Energy Surfaces and Dynamics Calculations*; Truhlar, D. G., Ed.; Plenum: New York, 1981; p 535.
(5) Huq, M. S.; Doverspike, L. D.; Champion, R. L. *Phys. Rev.* A **1983**, *27*, 2831.
(6) Zimmer, M.; Linder, F. *Chem. Phys. Lett.* **1992**, *195*, 153. Zimmer, M.; Linder, F. *J. Phys. B.* **1995**, *28*, 2671. Müller, H.; Zimmer, P.; Linder, F. *J. Phys. B.* **1996**, *29*, 4165.
(7) Gerlich, D. *Adv. Chem. Phys.* **1992**, *82*, 1.
(8) Mark, S.; Glenewinkel-Meyer, Th.; Gerlich, D. *Int. Rev. Phys. Chem.* **1996**, *15*, 283. Mark, S. *Ph.D. Thesis*, TU Chemnitz, 1996.
(9) Brehm, B.; Grosser, J.; Ruscheinski, T.; Zimmer, M. *Meas. Sci. Technol.* **1995,** *6*, 953.
(10) Gerlich, D. *J. Chem. Phys.* **1989**, *90*, 127.
(11) Chantry, P. J. *J. Chem. Phys.* **1971**, *55*, 2746.
(12) Beck, D. R.; Nicolaides, C. A. *Chem. Phys. Lett.* **1978**, *59*, 525.
(13) Haufler, E., Ph.D. Thesis, University Chemnitz, 1996.
(14) Boonenber, C. A.; Mayne, H. *Chem. Phys. Lett.* **1984**, *108*, 67.
(15) Aoiz, F. J.; Herrero, V. J.; Sáez Rábanos, V. *J. Chem. Phys.* **1991,** *94*, 7991.
(16) Westenberg, A. A.; de Haas, N. *J. Chem. Phys.* **1967**, *47*, 1393.
(17) Aoiz, F. J., to be published.